Hindawi
Mathematical Problems in Engineering
Volume 2017, Article ID 9456768, 13 pages
https://doi.org/10.1155/2017/9456768

Research Article

Shear Resistance Capacity of Interface of Plate-Studs Connection between CFST Column and RC Beam

Qianqian Wang,[1] Hua Ma,[1] Zhenbao Li,[1] Zhenyun Tang,[1] Haiyan Chen,[2] and Peng Li[2]

[1]*The Key Laboratory of Urban Security and Disaster Engineering, Ministry of Education, Beijing University of Technology, Beijing 100124, China*
[2]*Dalian Wanda Commercial Properties Co., Ltd., Beijing 100022, China*

Correspondence should be addressed to Zhenbao Li; lizb@bjut.edu.cn

Received 25 June 2017; Revised 6 September 2017; Accepted 26 September 2017; Published 25 October 2017

Academic Editor: Stefano Lenci

The combination of a concrete-filled steel tube (CFST) column and reinforced concrete (RC) beam produces a composite structural system that affords good structural performance, functionality, and workability. The effective transmission of moments and shear forces from the beam to the column is key to the full exploitation of the structural performance. The studs of the composite beam transfer the interfacial shear force between the steel beam and the concrete slab, with the web bearing most of the vertical shear force of the steel beam. In this study, the studs and vertical steel plate were welded to facilitate the transfer of the interfacial shear force between the RC beam and CFST column. Six groups of a total of 18 specimens were used to investigate the shear transfer mechanism and failure mode of the plate-studs connection, which was confirmed to effectively transmit the shear forces between the beam and column. The results of theoretical calculations were also observed to be in good agreement with the experimental measurements.

1. Introduction

The composite structural system produced by the combination of a concrete-filled steel tube (CFST) column and reinforced concrete (RC) beam is often used in China. The connection of the system is key to its application in high-rise buildings. Because the longitudinal reinforcements of the beam and the CFST column are uncoordinated around the connection of the system, the construction of the connection is quite complex. To address this issue, Fang et al. (2002) proposed the addition of a ring beam outside the CFST column in the connection area, with the longitudinal reinforcements of the slab beam anchored to the ring beam. The ring beam resists the bending moment of the RC beam by bearing the torsion. The connection surface between the beam and steel tube is bonded with a welded steel ring, which functions as a shear ring for transmission of the shear force. All the specimens of the proposed system used for seismic behavior experiments were found to exhibit good energy dissipation capacities [1]. Han et al. (2005) also proposed two types of connections between a CFST column and an RC beam. The first type comprised a ring steel plate, radial reinforcements, and steel brackets installed through the tubular core, while the second type consisted of ring reinforcements welded to the tube and steel brackets installed through the tubular core [2]. Zha et al. (2016) introduced a newly developed RC beam to a CFST column connection without welding on the construction site and presented a three-stage skeleton curve model of the system. The results of experiments and finite element analyses showed that the connection exhibited good ductility and the ability to dissipate energy and could be used to replace welded connections with reinforcement on the outer annular plate [3]. Chen et al. (2014, 2015) experimentally and analytically investigated the seismic and axial compressive behaviors of a new type of through-beam connection between a CFST column and RC beam, in which a strengthening RC ring beam was used to enlarge the connection zone to compensate for the possible decrease of the axial load capacity due to the discontinuity of the column in the connection zone [4, 5]. Zhou et al. (2017) proposed experimental, theoretical, and nonlinear FE methods for analyzing the structural behavior of three types

of connections between a circular CFST column and an RC beam under axial compression [6]. Kenji et al. (2005) proposed another type of connection in which the steel tube of the CFST column contained horizontal rectangular holes, into which the longitudinal reinforcements were inserted. A steel plate with holes for the reinforcements was then welded to the column and the nuts were tightened. Investigations revealed that the CFST column-RC beam connection exhibited excellent seismic performance and that the performance could be enhanced by increasing the degree of reinforcement anchorage at the center of the steel tube [7]. Further, Yuichi et al. (2000), Masato et al. (2002), and other researchers tested T-shaped and cross-shaped connections with longitudinal reinforcements welded to the diaphragm of the CFST column, with the purpose of applying them in track viaducts and subway stations. Low-cycle loads were implemented and the structural system was found to have rigid connections and satisfy design requirements [8, 9]. Based on strategies for maximizing economical filed construction, Kim et al. (2014) proposed several connections between a CFST column and an RC flat plate, and test results showed that they all exhibited a punching shear strength and connection stiffness that exceeded those of their RC flat plate counterparts [10]. Ju et al. (2013) compared three types of connections between a concrete-filled tube and flat plate and proposed a new connection detail wherein an anchored reinforcement bar connection was used in the longitudinal direction, a through reinforcement bar connection was used in the transverse direction, and a wing plate was welded around the CFST column to prevent punching shearing of the flat slab [11].

Indeed, several scholars at home and abroad have proposed different connection forms for CFST column-RC beam systems. The force-transfer mechanisms of the various connection forms differ and there is still no consensus for investigating their integrity. Nevertheless, there is still the need for the development of a CFST column and RC beam connection with good transmission of the beam moment and shear force.

Studs are used as flexible connectors in steel-concrete composite beams and substantial research has been devoted to their mechanical performance and shear capacity. Okada et al. (2006) used a push-out experiment and finite element analysis to investigate the mechanical characteristics of a group of studs and proposed a bearing capacity reduction factor for considering the effect of the group studs [12]. Shim et al. (2004) also performed a push-out experiment on the group studs shear connectors of a composite beam. The spacing of the studs was limited to no more than five times their diameter, and the resultant shear bearing capacity was assigned a coefficient [13]. Jorge et al. (2012) tested the shear behavior of stud connectors and proposed a formula for calculating the shear capacity, taking into consideration the longitudinal spacing and the length-to-diameter ratio of the studs [14]. Zhou et al. (2014) investigated the mechanical characteristics of the group stud shear connector of a steel anchor box. They conducted a finite element analysis of the effect of the group studs and their main influence factors and determined the bearing capacity reduction factor for calculating the shear capacity of the group studs connectors [15].

The vertical steel plate of a composite structure functions as the web of the structure and therefore bears the bulk of the shear force acting on the structure. In the design of the shear strength of the composite beam, all the sectional vertical shear forces are assumed to be borne by the web, in accordance with the Code of Design for Steel Structures GB50017-2003 [16], American Standard (American Institute of Steel Construction) [17], and European Code EC4 [18], which also include the formula for calculating the shear capacity of the web.

Based on the advantages that the transmission of shear forces by studs and vertical steel plates affords, this paper proposes a new connection between the RC beam and CFST column in which the longitudinal reinforcements are passed through the panel zone. The studs and vertical steel plate are welded to the tube wall to transfer the shear force. The shear behavior of the interface of the proposed connection was examined using six groups of a total of 18 specimens to establish the shear transfer mechanism and failure mode.

2. Configuration and Failure Mechanism of Plate-Studs Connection

Connection through the longitudinal reinforcements of a single-beam that passes through a CFST column is the method recommended by the Technical Code for Concrete-Filled Steel Tubular Structures GB50936-2014 [19]. In this type of connection, the bending moment of the beam is directly transferred to the concrete in the tube through the longitudinal reinforcements. This prevents the transmission of the bending moment to the concrete within the tube when the tube wall is separated from the concrete. The shearing force of the beam is transmitted to the CFST column through shear force resistance rings, annularly distributed steel brackets, and bearing pins welded to the tube wall. A shear force resistance ring is usually used together with a ring beam to transmit the shearing force of the beam; however, the CFST column is not sufficiently strong to bear the bending moment distribution and the stiffness of the connection is poor. Annularly distributed steel brackets enable the effective transfer of the shearing force of the beam to the CFST column. This, however, requires a significant amount of steel and welding work. In addition, the bearing pin that passes through the CFST column weakens the steel tube and also obstructs pouring of the concrete into the tube.

To solve the above problems, the plate-studs connection configuration shown in Figure 1 was developed. The connection includes the CFST column, RC beam, outer steel pipe, studs, and vertical steel plate. The single-bar holes in the steel tube correspond to the locations of the longitudinal reinforcements of the RC beam, with all the reinforcements passing through the holes. The outer steel plates are used to reinforce the holes, and the plate-studs are welded to the tube wall.

The force-transfer mechanism is as follows. The bending moment of the RC beam is directly transmitted to the CFST column by the force couple acting generated through the tensile force of the reinforcement and the compressive stress of the concrete in the compression area. The shearing force of the RC beam is also transferred to the CFST column

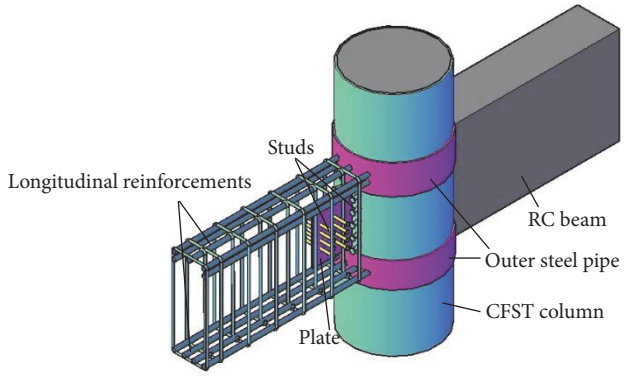

Figure 1: Configuration of the plate-studs connection.

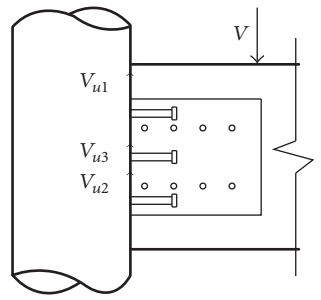

Figure 2: Composition of the interface shear resistance.

through the plate and studs. The advantage of this connection is the definite transmission path of the force and the minimal effect of the welding of the plate and studs on the stress concentration of the steel tube. This prevents tearing of the tube wall. The opening of the steel tube and the welding of the outer steel pipe and the plate and studs can be performed in the factory to minimize the amount of spot welding. In addition, the plate and studs are welded to the beam section and therefore do not affect the building aesthetics.

The key to designing a plate-studs connection is the determination of the ability of the plate and studs to transfer the shear force. Under the action of the shear force of the beam, the interface shear resistance is composed of three parts (see Figure 2):

$$V = V_{u1} + V_{u2} + V_{u3}, \quad (1)$$

where V is the shear force of the interface, V_{u1} is the natural shear bond force of the interface, V_{u2} is the shear force of the vertical plate, and V_{u3} is the shear force of the studs.

The failure mechanism and the composition of the bearing capacity of each part were investigated by shear resistance testing of the interface.

3. Experimental Design

3.1. Test Specimens. To investigate the shear resistance capacity of the interface of the plate-studs connection between the CFST column and RC beam, six groups of a total of 18 specimens were prepared, as shown in Figure 3. All the test specimens had the same dimensions. Their detailed parameters are given in Table 1. The steel tube was made from Q345B steel and had an outer diameter of 402 mm, thickness of 10 mm, and height of 600 mm. All the specimens were fabricated using C30-grade concrete based on the Chinese design code (2010). The measured strength parameters are given in Table 2. The cross-sectional dimensions of the RC beam were 250 × 200 × 750 mm. The longitudinal reinforcement consisted of 12 HRB400 steel bars of diameter 16 mm and stirrups with a 4C8@50 arrangement. The height of the interface was 450 mm. The studs welded to the interface were ML15 studs of diameter 13 mm and length 80 mm, with a yield strength of 388.75 MPa and ultimate tensile strength of 455.75 MPa. The horizontal and vertical spacing of the studs were 100 and 75 mm, respectively. The vertical steel plates were made from Q235 steel and were 225 mm long and 200 mm high. They had varying thicknesses of 6, 10, and 14 mm, respectively. The measured mechanical properties of the steel plates are presented in Table 3. Eight studs of diameter 10 mm were welded to each side of each vertical steel plate. The eight studs on each side of a plate had a 2 × 4 configuration with horizontal and vertical spacing of 50 and 100 mm, respectively.

The only vertical steel plates were those welded to the interfaces of specimens P1–P3, while plates and studs were welded to the interfaces of specimen PS1–PS3. The effects of the vertical steel plate thickness on the shear resistance of the interface were examined by comparing the P and PS group specimens, while the effects of the studs on the shear resistance of the interface were examined by comparing specimens P1 and PS1, P2 and PS2, and P3 and PS3, respectively.

3.2. Test Setup and Loading Protocol. Figure 4 shows the test setup. A 4000 kN electrohydraulic servo-loading system was used to apply a vertical load to the top of the RC beam corresponding to the interface. A balance frame was set at the top of the CFST column to prevent lifting of the specimen. All the specimens were tested monotonically up to their ultimate load under controlled vertical loading. Beyond the ultimate load, the loading was displacement-controlled. The main measurements included the relative slip between the concrete and tube wall at the center of the vertical steel plate. The measurement points are shown in Figure 5.

4. Test Results

4.1. Failure Process and Mode. The experimental observations and analysis of the test results for the six groups of the 18 specimens revealed that all the specimen failures were bond-splitting failures. As shown in Figure 5, the failure process of a specimen was observed using a distance of 50 mm over the surface of the concrete along the height of the interface as the unit grid. The grid cells were identified by the letters A–E horizontally, with E lying close to the interface, and numbers 1–9 from the top to the bottom.

(1) Only Welded Vertical Steel Plate at the Interface (P1–P3 Specimens). In the initial stage of the loading, there was no crack in any of the specimens. When the load reached 15%–20% of the ultimate load, vertical microcracks appeared

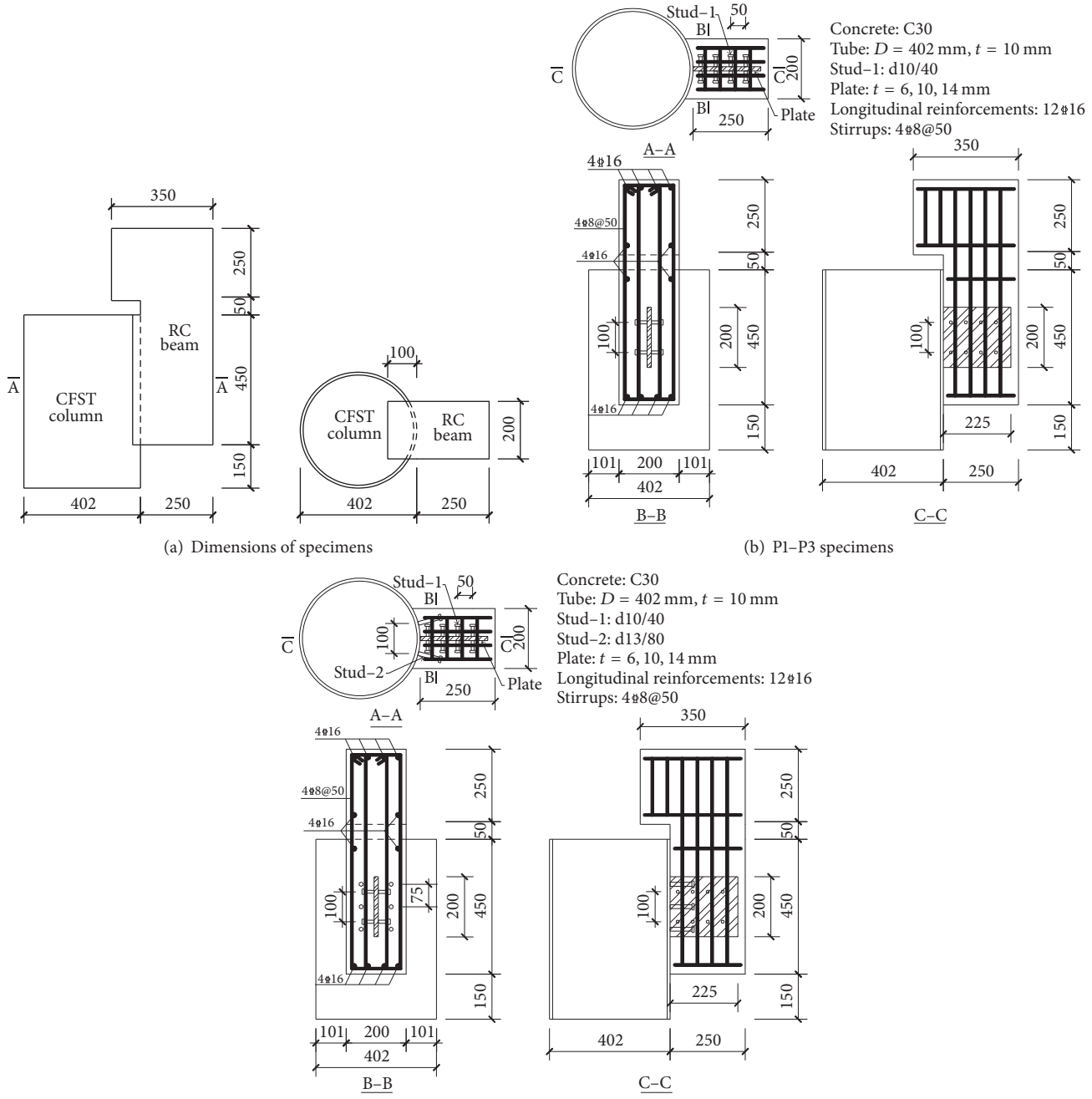

(a) Dimensions of specimens

(b) P1–P3 specimens

(c) PS1–PS3 specimens

Figure 3: Details of the test specimens (all dimensions are in mm).

Table 1: Specimen parameters.

Configuration of the interface	Specimen group	Number of specimens	Dimensions of the vertical steel plate Length × height × thickness (mm)	Arrangement of the interface studs
Only vertical steel plate	P1	3	225 × 200 × 6	No studs
	P2	3	225 × 200 × 10	No studs
	P3	3	225 × 200 × 14	No studs
Plate-studs	PS1	3	225 × 200 × 6	3 × 2
	PS2	3	225 × 200 × 10	3 × 2
	PS3	3	225 × 200 × 14	3 × 2

Table 2: Mechanical properties of the concrete.

Strength grade	Cube compressive strength f_{cu}/MPa	Prism compressive strength f_c/MPa	Elastic modulus E_c/MPa
C30	34.1	25.6	31050

Table 3: Mechanical properties of the vertical steel plate.

Thickness/mm	Yield strength f_y/MPa	Tensile strength f_s/MPa	Elastic modulus E_s/GPa
6	245.5	368.5	206
10	268.5	387.2	206
14	310.2	420.7	206

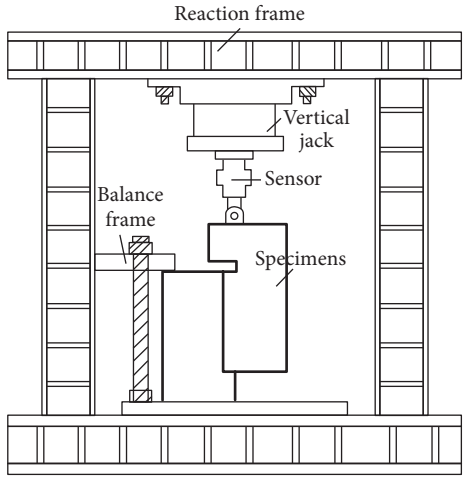

Figure 4: Test setup.

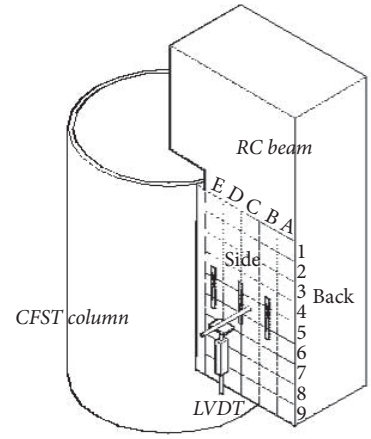

Figure 5: Instrumentation layout.

at the interface between the tube wall and the concrete. At 75%–85% of the ultimate load, a fine horizontal crack appeared at the back of the concrete above the vertical steel plate and extended to the side. At the ultimate load, slanting cracks were seen along the upper part of the beam, reaching to the lower part of the free end. A vertical crack was also generated on the back surface of the beam. Under subsequent loading with displacement control, the cracks apparently expanded and a number of new diagonal cracks emerged from the first diagonal crack. A diagonal crack eventually became the main crack, and some of the concrete within the vertical steel plate was chipped off. As shown in Figure 6, nine specimens from three groups exhibited this failure mode.

(2) Welded Plate-Studs at the Interface. In the initial stage of the loading, there was no crack in any of the specimens. When the load reached 14%–18% of the ultimate load, vertical microcracks appeared at the interface between the tube wall and the concrete. At 55%–75% of the ultimate load, two fine horizontal cracks appeared at the back of the concrete and extended to the side. One of them was at the top of the vertical steel plate, while the other was within the range of the plate. A diagonal crack also appeared within the range of the vertical steel plate under the same load. When the load reached 90% of the ultimate load, a number of slanting cracks appeared within the range of the vertical steel plate and expanded upward and downward. Horizontal cracks also appeared at the points where the studs were welded to the tube wall, while vertical cracks appeared at the back of the beam. Under subsequent loading with displacement control, the cracks apparently expanded and the concrete behind the vertical steel plate was chipped off. As shown in Figure 7, nine specimens from three groups exhibited this failure mode.

The cracking load of the concrete, the ultimate load of the specimen, and the slip corresponding to the ultimate load are presented in Table 4.

4.2. Load-Slip Curves. Relative slip between the concrete and the tube wall at the center of the vertical steel plate occurred under loading. The obtained load-slip curves are shown in Figure 8. It can be seen that there is no relative slip between the concrete and the tube wall until the load reaches 15%–20% of the ultimate load. This indicates that the RC beam and CFST column are well bonded and function in tandem. Relative slip begins under 55%–80% of the ultimate load, although it is very small. Thereafter, the growth rate of the slip gradually increases. At 90% of the ultimate load, the slip rapidly develops. Beyond the ultimate load, the load decreases sharply. The load tends to stabilize after dropping to 45%–40% of the ultimate load, but the slip continues to develop under plastic conditions.

Table 4: Test results.

Specimen number	V_0/kN	V_1/kN	V_u/kN	S_u/mm	V_1/V_u%	$V_{u,av}$/kN	$V_{1,av}/V_{u,av}$%
P1-A	73	305	387.0	1.40	79		
P1-B	71	285	396.2	3.45	72	388.9	79
P1-C	77	340	383.4	2.31	87		
P2-A	71	335	398.6	1.23	84		
P2-B	62	315	363.3	1.67	86	393.4	82
P2-C	67	315	418.4	1.02	75		
P3-A	64	319	429.3	1.27	74		
P3-B	65	319	433.3	2.00	74	431.3	77
P3-C	69	360	431.3	0.99	83		
PS1-A	69	345	381.2	0.71	90		
PS1-B	74	298	407.7	0.48	73	390.9	78
PS1-C	66	275	383.8	1.23	72		
PS2-A	75	302	437.0	1.40	69		
PS2-B	74	254	446.6	1.38	57	448.1	60
PS2-C	76	250	460.6	1.55	54		
PS3-A	71	251	468.5	0.93	54		
PS3-B	65	250	427.6	1.18	58	458.3	55
PS3-C	72	260	478.8	1.12	54		

V_0: bonding damage load, V_1: initial cracking load, V_u: ultimate load, S_u: slip corresponding to the ultimate load, $V_{u,av}$: average ultimate load, and $V_{1,av}$: average initial cracking load.

5. Analysis of Results

5.1. Typical Load-Slip Curve. Based on the above specimen analyses, the typical load-slip curve, which gives an insight into the shear resistance of the interface specimens, was obtained, as shown in Figure 9. It can be seen that the curve comprises four stages, namely, the no-slip stage, the increasing bond slip stage, the rapid decrease stage, and the stable stage.

(1) No-Slip Stage (OA). In this stage, the natural bond force between the steel tube wall and the concrete bears the vertical load, and there is no relative slip between the steel plate and the concrete. The RC beam and CFST column are well bonded under this condition. When the cement gel at the interface is cut, the natural bond force is overcome, and there is relative slip between the tube wall and the concrete. The studs welded to the vertical steel plate strengthen the bond between the vertical steel plate and the concrete, delaying internal cracking of the concrete and thereby reducing the relative slip between the tube wall and the concrete. The load at this stage is 55%–80% of the ultimate load.

(2) Increasing Bond Slip Stage (AB). When the load reaches P_1, the specimen mainly depends on the friction between the tube wall and the concrete, as well as the shear resistance of the steel plate, to transfer the load. However, due to gradual cracking of the concrete, the growth rate of the friction gradually decreases, resulting in the sliding increasing faster than the load and hence increasing nonlinearity of the load-slip curve.

(3) Rapid Decrease Stage (BC). When the load reaches the ultimate load, the relative slip between the tube wall and concrete significantly develops, with the crack width increasing. Due to the crushing of the concrete under the studs and splitting of the back of the RC beam, the load rapidly decreases.

(4) Stable Stage (CD). After the decrease of the load to a certain level, the internal cracks at the interface between the vertical steel plate and the concrete basically stabilize. At this stage, the concrete crystal has been fully crushed and the normal stress, frictional resistance, and mechanical interlocking of the interface are almost constant. However, the slip continues to develop, resulting in unstable plastic flow conditions in the bond.

The specimens with only welded vertical steel plates at their interface obviously exhibit the above four stages. In the case of the specimens with welded plate-studs at their interface, the full development of the concrete cracks causes the slope of the rapid decrease stage to be steeper, and the stable stage is not obvious.

5.2. Effect of Vertical Steel Plate Thickness. The effect of the vertical steel plate thickness on the load-slip curve is shown in Figure 10. From Figure 10 and Table 4, it can be seen that the shear resistance of the interface increases with increasing thickness of the vertical steel plate. In addition, the time required for the initial cracking of the concrete shortens and the slope of the rapid decrease stage increases.

5.3. Effect of Studs. Figure 11 shows the effect of the welded studs on the load-slip curve for a given vertical steel plate thickness. From the figure, it can be seen that welding of the studs improves the shear resistance capacity of the interface. Comparison of the PS1 and P1, PS2 and P2, and PS3 and P3

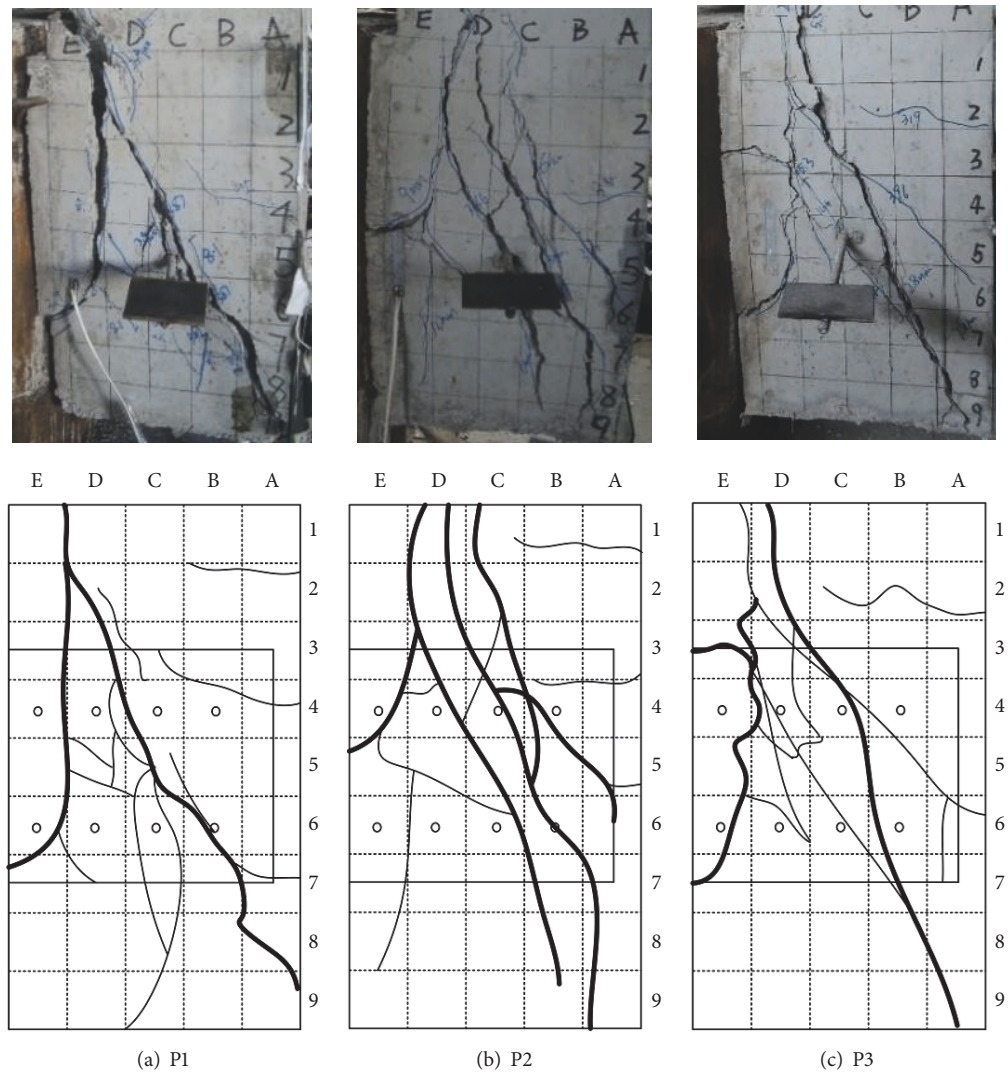

(a) P1 (b) P2 (c) P3

Figure 6: Failure modes of the P1–P3 specimens.

specimens reveals improvements of 0.5%, 13.9%, and 6.3%, respectively. The performance of the specimen with a 10 mm thick vertical plate and 3 × 2 studs is optimal.

6. Calculation of Shear Resistance Capacity of Interface

6.1. Shear Resistance of Interface with Only Welded Vertical Steel Plate. Under the action of the vertical load V, the interface shear resistance of the P1–P3 specimens (with only the welded vertical steel plate at the interface) had two components, namely, the natural bond force of the interface and the shear capacity of the vertical steel plate. This is illustrated in Figure 2.

$$V = V_{u1} + V_{u2}. \tag{2}$$

The possible failure modes of the specimens of the three groups are shearing failure of the weld seam of the vertical steel plate root, shearing failure of the vertical steel plate root, and splitting failure of the concrete. The shear capacity of the interface is the least among the bearing capacities under the three failure modes.

With regard to the bond shear strength between the steel tube and the concrete outside the tube, Qian et al. (2015) suggested a value of 0.7 MPa [20]. On this basis, the natural shear bond force of the interface is given by

$$V_{u1} = \tau_u lh, \tag{3}$$

where τ_u is the bond strength between the steel tube and the concrete and l and h are, respectively, the length and height of the interface.

Under the first two of the above failure modes, the shear capacity of the vertical steel plate can be calculated according to the Design Code for Steel Structures GB50017-2003. In the case of concrete splitting failure, the shear capacity of the vertical steel plate consists of two parts, namely, the shear strength determined by the local compressive bearing capacity of the concrete at the top of the vertical steel plate

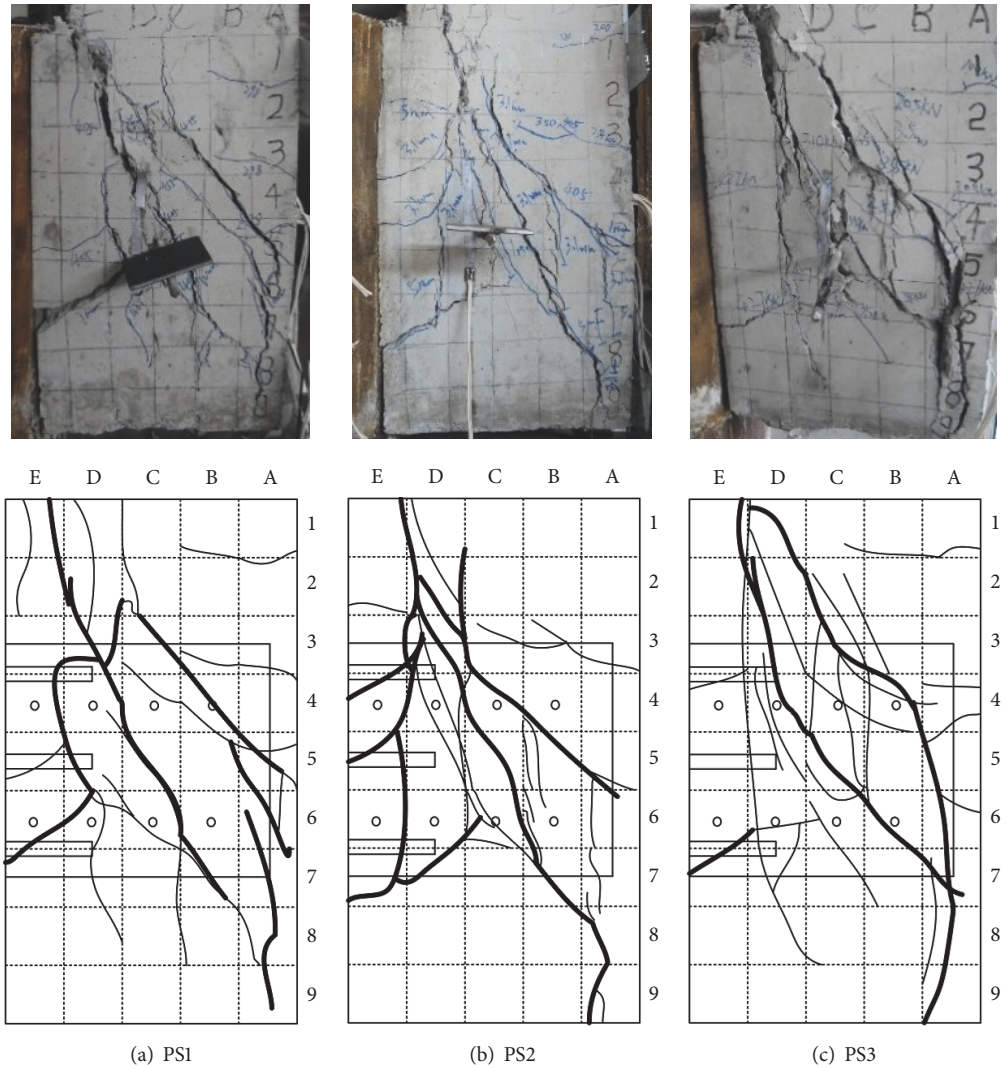

Figure 7: Failure modes of the PS1–PS3 specimens.

and the shearing force of the concrete crushed by the studs welded to the vertical steel plate. This is expressed by

$$V_{u2} = V_{u21} + V_{u22}. \tag{4}$$

The local compression bearing capacity of the concrete at the top of the vertical steel plate is calculated as follows:

$$V_{u21} = \beta f_c A_1, \tag{5}$$

where A_1 is the action area of the local pressure and β is the local compressive strength coefficient of the concrete, considered to be 1.5.

The shearing force of the concrete crushed by the studs welded to the vertical steel plate is calculated as follows:

$$V_{u22} = 0.43 A_s \eta \sqrt{E_c f_c} \le 0.7 \eta A_s f_u, \tag{6}$$

where A_s is the sum of the cross-sectional areas of the studs, E_c is the elastic modulus of the concrete, f_c is the axial compressive strength of the concrete, f_u is the ultimate tensile strength of the studs, and η is the reduction coefficient of the group stud effect, which can be calculated by the following equations [7]:

$$\begin{aligned} 3 \le d_s < 13: &\quad \text{Concrete C25/30, } \eta = 0.023 d_s + 0.70 \\ &\quad \text{Concrete C30/37, } \eta = 0.021 d_s + 0.73 \\ &\quad \text{Concrete C40/50, } \eta = 0.016 d_s + 0.80 \\ &\quad \text{Concrete C50/60, } \eta = 0.013 d_s + 0.84 \\ d_s \ge 13: &\quad \text{Concrete C25/30–C50–60, } \eta = 1, \end{aligned} \tag{7}$$

where d_s is the ratio of the spacing to the stud diameter.

In this paper, the failure mode of the test specimen with only the vertical steel plate at the interface is bond-splitting failure of the concrete, and the shear capacity can be calculated using

$$V = V_{u1} + V_{u21} + V_{u22}. \tag{8}$$

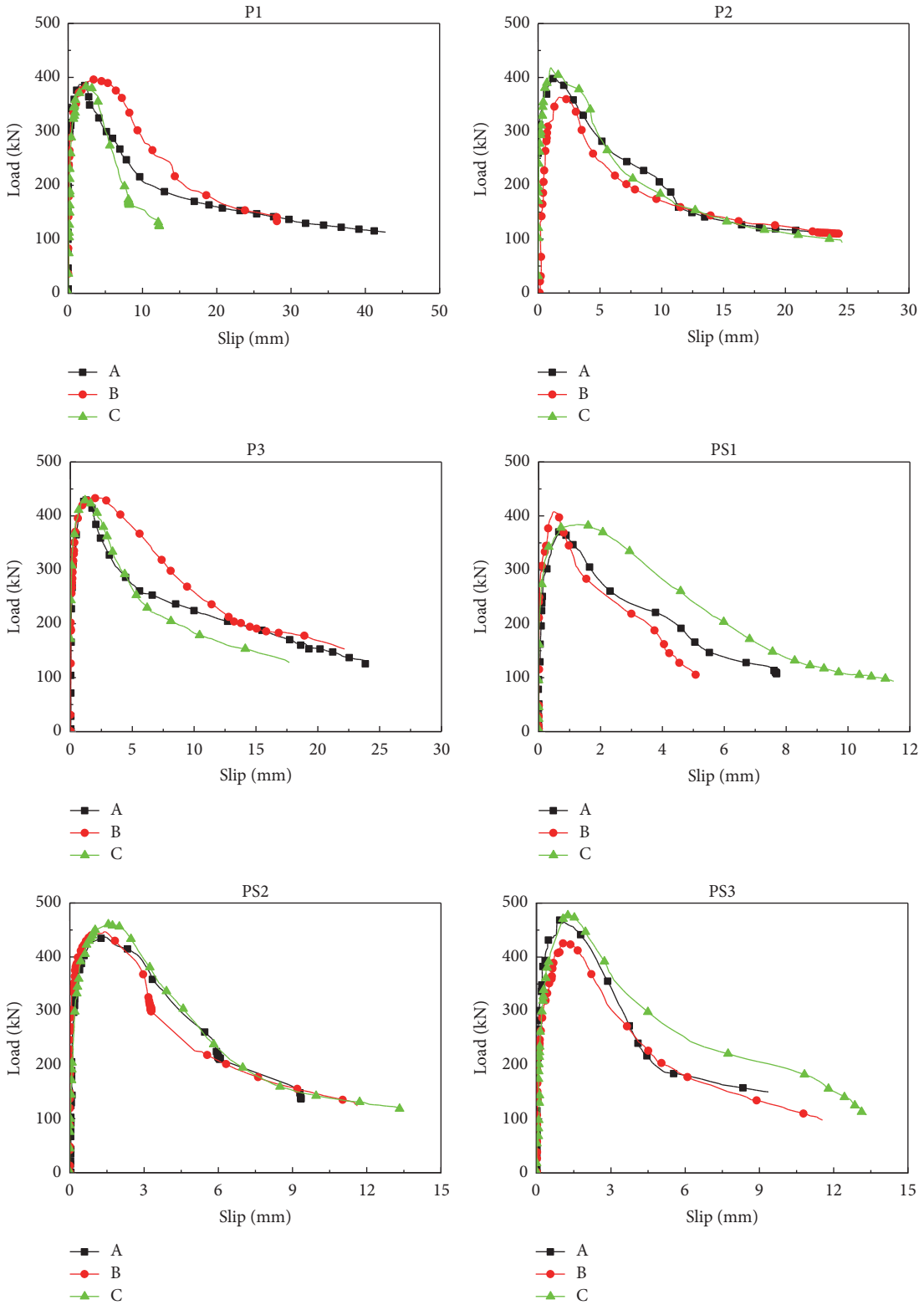

Figure 8: Load-slip curves.

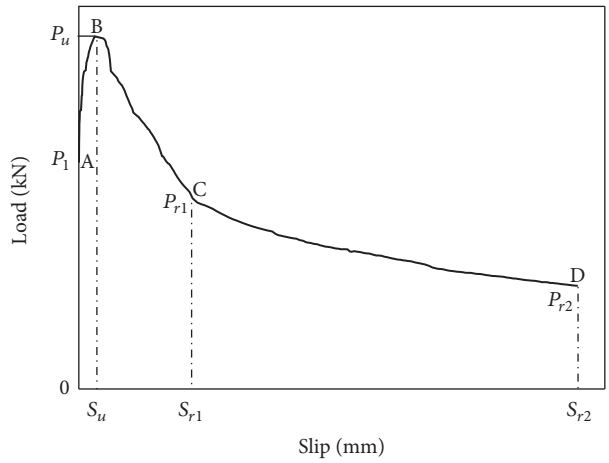

Figure 9: Typical load-slip curve.

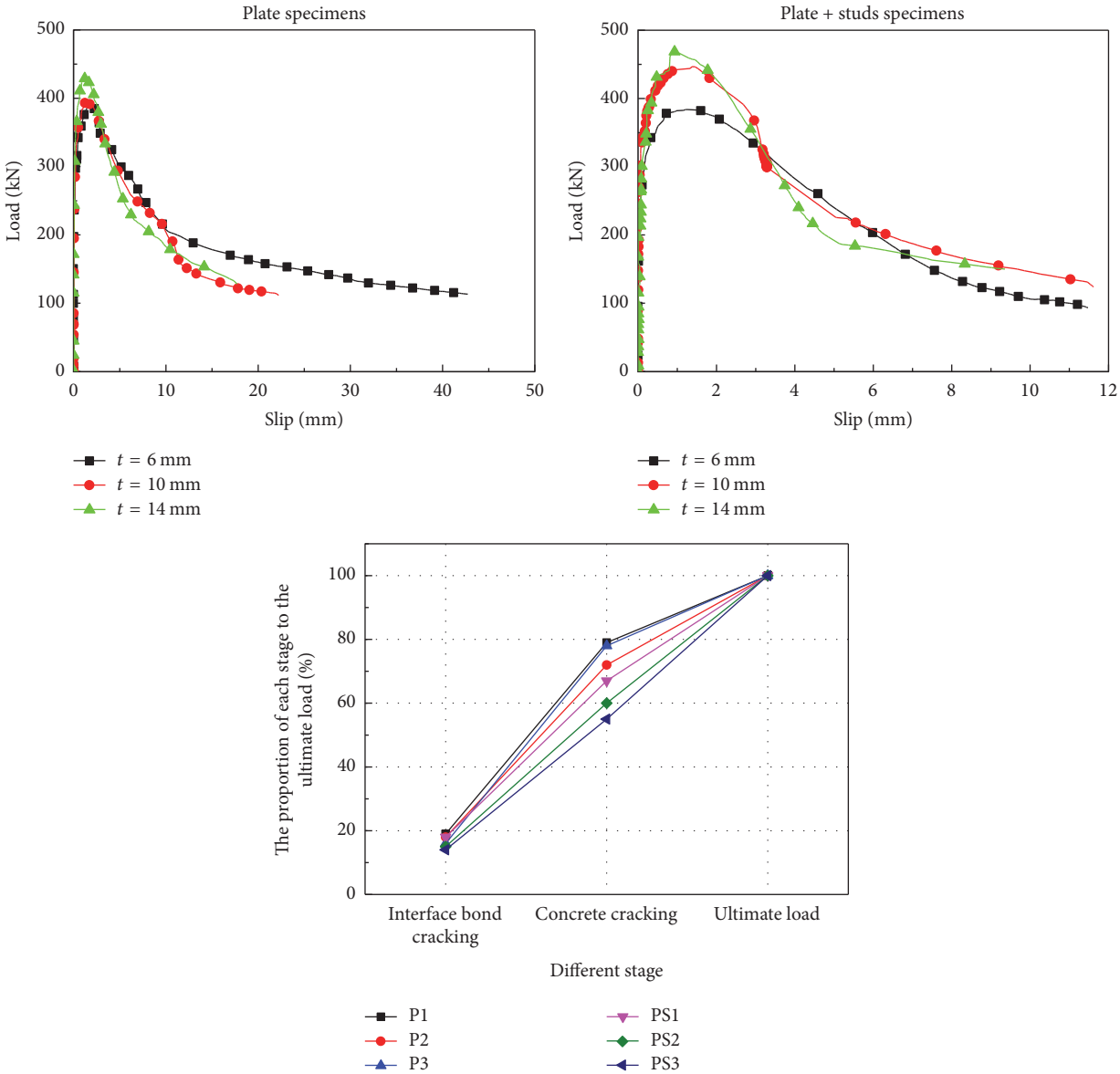

Figure 10: Effects of the vertical steel plate thickness.

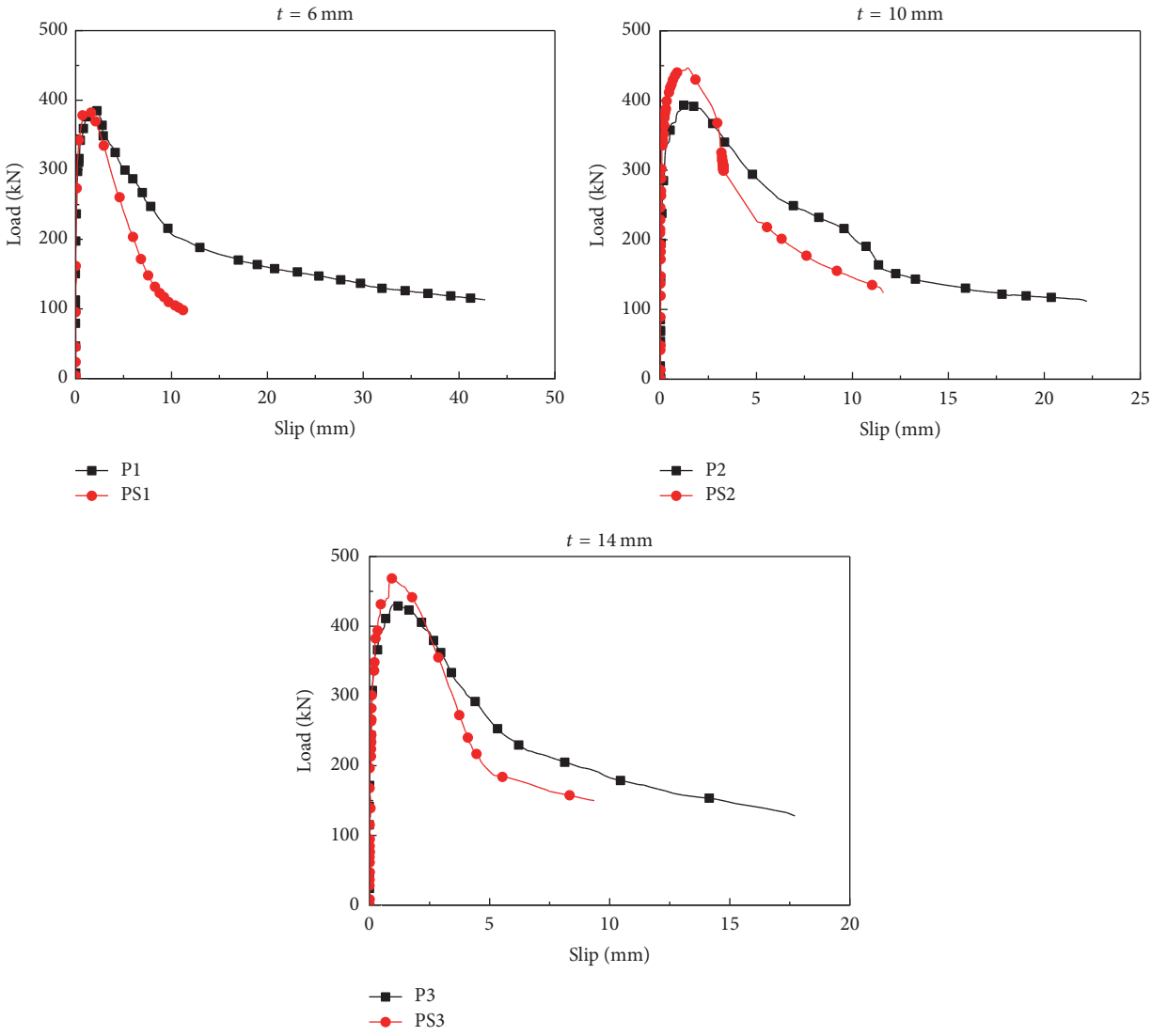

Figure 11: Effect of the welded studs.

The experimentally determined and calculated shear forces are presented in Table 5, from which good agreement can be observed between the two sets of results. Taking into account the horizontal and longitudinal group arrangement effect, $\eta = 0.7$.

6.2. Shear Resistance Force of Interface with Welded Plate-Studs. The PS1–PS3 specimens had the plate-studs at their interface. The added studs had three effects: inducement of concrete splitting tensile failure; local crushing failure of the concrete under the studs; and stud shear failure. The shear capacity of the studs is the least among the bearing capacities under the three failure modes.

The shearing force of the studs under concrete splitting failure is given by

$$V_{u3} = f_t A_2, \tag{9}$$

where A_2 is the splitting area and f_t is the tensile strength of the concrete.

Under local crushing failure of the concrete and stud shear failure, the shearing force of the studs is given by (6).

In this study, the failure mode of the test specimens with welded plate-studs at their interface was bond-splitting failure of the concrete, and the shear capacity was calculated using

$$V = V_{u1} + V_{u21} + V_{u22} + V_{u3}. \tag{10}$$

The experimentally determined and calculated shear forces are presented in Table 5, which reveals good agreement between the two sets of results.

Care should be taken so that (2)–(10) are suitable for the specimens that exhibit bond-splitting failure.

7. Conclusions

In the present study, a new connection of the longitudinal reinforcements of the RC beam was developed, wherein the reinforcements were passed through the panel zone of the

Table 5: Experimentally determined and calculated shear forces.

Specimen group	V_e/kN	V_c/kN	V_c/V_e	V_{u1} (V_{u1}/V_c)	V_{u21} (V_{u21}/V_c)	V_{u22} (V_{u22}/V_c)	V_{u3} (V_{u3}/V_c)
P1	388.87	363.45	0.94	65.31 (0.18)	51.84 (0.14)	246.3 (0.68)	0
P2	393.44	397.45	1.01	64.75 (0.16)	86.4 (0.22)	246.3 (0.62)	0
P3	431.32	431.45	1.00	64.19 (0.15)	120.96 (0.28)	246.3 (0.57)	0
PS1	390.90	423.65	1.08	65.31 (0.16)	51.84 (0.12)	246.3 (0.58)	60.2 (0.14)
PS2	448.06	457.65	1.02	64.75 (0.14)	86.4 (0.19)	246.3 (0.54)	60.2 (0.13)
PS3	458.32	491.65	1.07	64.19 (0.13)	120.96 (0.25)	246.3 (0.50)	60.2 (0.12)

V_e: experimentally determined value, V_c: calculated value, V_c/V_e: the ratios of the calculated value to the experimentally determined bearing capacity, and V_{ui}/V_c: the contribution of each component to the ultimate strength of the specimen (the values in parentheses).

connection between the CFST column and RC beam. Studs and a vertical steel plate were welded to the tube wall to transfer the shear force of the RC beam to the CFST column. The shear resistance capacity of the interface was investigated using six groups of a total of 18 specimens. The following is a summary of the major findings of the study.

(1) When the concrete of the RC beam is C30, the failure mode is bond-splitting failure of the concrete.

(2) The interface of the plate-studs connection proposed in this paper has a high shear bearing capacity, and the corresponding peak load is within 1.5 mm. This indicates that, through a reasonable design, the welded plate and studs at the interface can be used to effectively transfer the shear force of the RC beam to the CFST column.

(3) An equation for calculating the shear bearing capacity of the connection interface between the CFST column and RC beam was derived, and its results were found to be in good agreement with experimental measurements.

Conflicts of Interest

The authors declare no conflicts of interest.

Authors' Contributions

Zhenbao Li, Qianqian Wang, and Hua Ma conceived the idea of the study. Qianqian Wang, Zhenyun Tang, Haiyan Chen, and Peng Li conducted the experiments and analyzed the results. Qianqian Wang and Zhenyun Tang translated the article, analyzed the results, and formatted the manuscript. All the authors interpreted and discussed the experimental results and provided substantive comments.

Acknowledgments

This research was funded by the National Key Basic Research and Development Program of China (Grant no. 2016YFC0701100) and the Dalian Wanda Commercial Real Estate Co., Ltd.

References

[1] X.-D. Fang, S.-Y. Li, J.-R. Qian, and R.-Q. Yang, "Experimental research on seismic behavior of concrete filled steel tubular column-ring beam joint under cyclic loading," *Journal of Building Structures*, vol. 23, no. 6, p. 10, 2002.

[2] X.-L. Han, R.-B. He, and J. Jing, "Experimental research on CFST connections with ring plate and steel corbels through the core," *Industrial Construction*, vol. 35, no. 11, pp. 21–24, 2005.

[3] X.-X. Zha, C.-Y. Wan, H. Yu, and J.-B. M. Dassekpo, "Seismic behavior study on RC-beam to CFST-column non-welding joints in field construction," *Journal of Constructional Steel Research*, vol. 116, pp. 204–217, 2016.

[4] Q.-J. Chen, J. Cai, M.-A. Bardford, X.-P. Liu, and Z.-L. Zuo, "Seismic behaviour of a through-beam connection between concrete-filled steel tubular columns and reinforced concrete beams," *Engineering Structures*, vol. 80, pp. 24–39, 2014.

[5] Q.-J. Chen, J. Cai, M.-A. Bardford, X.-P. Liu, and Y. Wu, "Axial Compressive Behavior of Through-Beam Connections between Concrete-Filled Steel Tubular Columns and Reinforced Concrete Beams," *Journal of Structural Engineering (United States)*, vol. 141, no. 10, Article ID 04015016, 2015.

[6] X.-H. Zhou, G.-Z. Cheng, J.-P. Liu, D. Gan, and Y. F. Chen, "Behavior of circular tubed-RC column to RC beam connections under axial compression," *Journal of Constructional Steel Research*, vol. 130, pp. 96–108, 2017.

[7] T. Kenji, E. Hiroshi, K. Hideyuki, and Y. Hisayuki, "Experimental study of hybrid structures composed of CFT-column and RC beam," *Mitsui Sumitomo Construction Institute of Technology Report*, vol. No. 3, pp. 113–118, 2005.

[8] L. Yuichi, K. Hiroshi, F. Mutsuo, and M. Nobuyuki, "Load carrying capacity of joint part between CFT column and RC beam with fixed plate," vol. 22, pp. 1153–1158, 2000.

[9] Y. Masato, N. Masaaki, and N. Okano, "Load Test and 3 - D Finite Element Analysis of the Joints of CFT Columns and RC Beams," in *Proceedings of the Japan Concrete Institute*, vol. 24, pp. 415–420, 2002.

[10] J.-W. Kim, C.-H. Lee, and T. H.-K. Kang, "Shearhead reinforcement for concrete slab to concrete-filled tube column connections," *ACI Structural Journal*, vol. 111, no. 3, pp. 629–638, 2014.

[11] Y. K. Ju, Y. C. Kim, and J. Ryu, "Finite element analysis of concrete filled tube column to flat plate slab joint," *Journal of Constructional Steel Research*, vol. 90, pp. 297–307, 2013.

[12] J. Okada, T. Yoda, and J. Lebet, "A study of the grouped arrangements of stud connectors on shear strength behavior," *Structural Engineering/Earthquake Engineering*, vol. 23, no. 1, pp. 75s–89s, 2006.

[13] C.-S. Shim, P.-G. Lee, and T.-Y. Yoon, "Static behavior of large stud shear connectors," *Engineering Structures*, vol. 26, no. 12, pp. 1853–1860, 2004.

[14] J. D.-B. Rocha, E.-M. Arrizabalaga, R.-L. Quevedo, and C. A.-R. Morfa, "Behavior and strength of welded stud shear connectors

in composite beam," *Revista Facultad de Ingeniería Universidad de Antioquia*, vol. 63, pp. 93–104, 2012.

[15] X.-H. Zhou, W.-R. Lu, J. Di, F.-J. Qin, and M. Zhao, "Group studs effect and shear strength calculation method for group studs shear connector of steel anchor box," *China Journal of Highway and Transport*, vol. 27, no. 12, pp. 33–45, 2014.

[16] Ministry of Construction of the People's Republic of China. GB 50017-2003, Code for Design of Steel Structures, Chinese Planning Press, Beijing, China, 2003.

[17] AISC. Load and Resistance Factor Design (LRFD) Specifications for Structural Steel Buildings, American Institute of Steel Construction, Chicago, IL, USA.

[18] CEN. EN1994-1-1:2004, Design of Composite Steel and Concrete Structures, Part 1.1: General Rules and Rules for Buildings, European Committee for Standardization, Brussels, Belgium, 2004.

[19] Ministry of Housing and Urban-Rural Development of the People's Republic of China (MOHURD). GB 50936-2014, Technical Code for Concrete Filled Steel Tubular Structures, China Architecture & Building Press, Beijing, China, 2014.

[20] J. R. Qian, Z. Z. Zhao, and X. D. Ji, "Test study on shear-bond capacity of steel tube-out of tube concrete interface," *Building Structure*, vol. 45, no. 3, pp. 12–16, 2015.